第 34 卷第 9 期 武 汉 工 程 大 学 学 报 Vol. 34 No. 9
2012 年 09 月 J. Wuhan Inst. Tech. Sep. 2012

文章编号:1674－2869(2012)09－0054－05

针束型回热器熵产率的分析

杨志春[1],吴 锋[2],余仕成[2]
(1. 海军驻武汉 438 厂军事代表室,湖北 武汉 430064;2. 武汉工程大学理学院,湖北 武汉 430074)

摘 要:回热器是热声装置的关键部件,在多种具有规则流道的回热器结构中,针束型结构是综合性能最优的结构. 针对针束型回热器参数优化问题,建立了以最小熵产率为目标的优化模型,研究基于不可逆性的回热器参数优化方法. 通过分析工质在回热器内振荡时由于与固壁的换热和黏性扩散导致的热动力学上不可逆性,对工质在针束型回热器内运动时的熵产率进行了理论分析和数值计算. 计算获得了回热器截面分布和截面平均熵产率表达式,分析了针束型回热器中不同位置截面分布熵产率的变化规律,分析了温度梯度对截面平均熵产率的影响,获得了给定特征尺寸截面平均熵产率最小时的最优频率和最优阻抗比.

关键词:熵产率;优化频率;针束型回热器;热声;不可逆性
中图分类号:TB131 **文献标识码**:A **doi**:10.3969/j. issn. 1674-2869. 2012. 09. 012

0 引 言

热声发动机和制冷机没有或者很少有运动部件,并且使用环境友好气体作为工质,以上突出优点使其在近年来备受关注[1]. 回热器是热声热机的关键部件[2-3],实际热声装置中使用了多种结构形式的回热器包括平行板结构、圆孔结构和钢丝型结构等[4-5]. Swift 等[6-7]引入了一种被称为针束结构的新型回热器:针束型结构如图 1 所示,在回热器轴向位置平行布置多根细针,单根针半径为 r_d,每根针处于一个正六边形流道中心. 理论与实验均已证明针束型回热器结构优于其它规则几何结构的回热器[8].

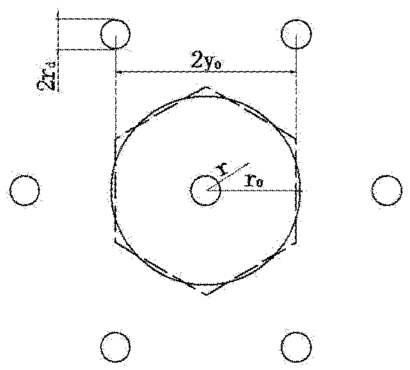

图 1 针束结构回热器横截面局部示意图

Fig. 1 A schematic diagram of the pin-array stack

工质在回热器内振荡时的换热和黏性损耗会导致不可逆损失,这种不可逆损失可以通过熵产率[9-10]来分析. 文献[11－16]对热声装置不可逆性进行了分析,但这些研究仅仅集中于单板、平行板或钢丝型回热器以及换热器. 本文对针束回热器中由换热和黏性耗散导致的熵产率进行了分析,研究了间距、尺寸、角频率、温度梯度和阻抗比等参数对熵产率的影响.

1 理论分析

根据针束型结构特点利用柱面坐标系(x,r,θ)进行分析,其中坐标 x 表示声波传播方向(针束沿此方向排列). 为便于计算,如图 1 所示:Swift 等[6-7]将每根针对应的正六边形流道等效为一个面积相等的半径为 r_0 的圆形流道,满足:$r_0=\sqrt{2\sqrt{3}/\pi}\,y_0\approx1.05y_0$,其中 y_0 为相邻针束 1/2 中心距.

线性化动量守恒方程为[4]

$$i\omega\rho_0u_1=-\frac{dp_1}{dx}+\mu\nabla^2u_1 \quad (1)$$

中 $i=\sqrt{-1}$,p_1 为工质的复压力振幅,ω 为角频率,ρ_0 为工质平均密度,u_1 为工质的复速度振幅,μ 为工质动力黏度.

在无滑边界条件下,有:

$$u_1(r_d)=0 \quad (2)$$

在针的表面,对称边界条件下:

$$\nabla_{\perp}u_1(hexagon)=\frac{\partial u_1(r_0)}{\partial r}=0 \quad (3)$$

收稿日期:2012-09-10
基金项目:国家自然科学基金项目(51176143);中国科学院低温工程学重点实验室开放课题(yoas011101)
作者简介:杨志春(1982-),男,江西星子人,工程师,博士. 研究方向:热能动力装置优化.

其中 $\nabla_\perp$ 表示在图 1 所示单元上与该六边形单元边界垂直方向求导.

连续性方程为:

$$\frac{\partial p_1}{\partial t}+\rho_0\frac{\partial u_1}{\partial x}=0 \quad (4)$$

其中 c_p 为工质的复密度振幅.

线性化能量方程为:

$$\rho_0 c_p(\mathrm{i}\omega T_1+u_1\frac{\mathrm{d}T}{\mathrm{d}x})-\mathrm{i}\omega T_0\beta p_1=k[\frac{1}{r}\frac{\partial}{\partial r}(r\frac{\partial T_1}{\partial r})] \quad (5)$$

其中 c_p 为比定压热容,T_1 为复温度振幅,$\mathrm{d}T/\mathrm{d}x$ 为温度梯度,T_0 为平均温度,β 为等温膨胀系数,k 为工质导热系数.

线性化状态方程为:

$$p_1=\rho_1 a^2+\frac{\rho_0}{\beta T_0}(1-\gamma)T_1 \quad (6)$$

其中 a 为工质绝热声速,γ 为比热比.

由公式(1)-(6)可得:

$$T_1=\frac{T_0\beta}{\rho_0 c_p}p_1(x)(1-f_k)+\frac{\mathrm{i}u_1(x)}{\omega}\times \frac{\mathrm{d}T_0}{\mathrm{d}x}(1+\frac{\sigma}{1-\sigma}f_\mu-\frac{1}{1-\sigma}f_k) \quad (7)$$

$$u_1=u_1(x)[1-\frac{Y_1(z_{0\mu})J_0(z_\mu)-J_1(z_{0\mu})Y_0(z_\mu)}{Y_1(z_{0\mu})J_0(z_{d\mu})-J_1(z_{0\mu})Y_0(z_{d\mu})}]=-\frac{1}{\mathrm{i}\omega\rho_0}\frac{\mathrm{d}p_1}{\mathrm{d}x}[1-\frac{Y_1(z_{0\mu})J_0(z_\mu)-J_1(z_{0\mu})Y_0(z_\mu)}{Y_1(z_{0\mu})J_0(z_{d\mu})-J_1(z_{0\mu})Y_0(z_{d\mu})}] \quad (8)$$

其中

$$f_k=\frac{Y_1(z_{0k})J_0(z_k)-J_1(z_{0k})Y_0(z_k)}{Y_1(z_{0k})J_0(z_{dk})-J_1(z_{0k})Y_0(z_{dk})} \quad (9)$$

$$f_\mu=\frac{Y_1(z_{0\mu})J_0(z_\mu)-J_1(z_{0\mu})Y_0(z_\mu)}{Y_1(z_{0\mu})J_0(z_{d\mu})-J_1(z_{0\mu})Y_0(z_{d\mu})} \quad (10)$$

其中 J_0 和 J_1 分别表示零阶和一阶 Bessel 函数,Y_0 和Y_1 分别表示零阶和一阶 Neumann 函数,$z_\mu=r\cdot\sqrt{-i\omega\rho_0/\mu}=(\mathrm{i}-1)r/\delta_\mu$,$z_{0\mu}=(\mathrm{i}-1)r_0/\delta\mu$,$z_{d\mu}=(\mathrm{i}-1)r_d/\delta_\mu$,$z_k=(\mathrm{i}-1)r/\delta_k$,$z_{0k}=(\mathrm{i}-1)r_k/\delta_k$,$z_{dk}=(\mathrm{i}-1)r_d/\delta_k$,$\delta_\mu$ 为工质的黏性渗透深度,δ_k 为工质的热渗透深度.

单位质量工质能量方程为

$$\frac{\mathrm{d}E}{\mathrm{d}t}+p\frac{\mathrm{d}V}{\mathrm{d}t}=V\phi-V\nabla\cdot\vec{q} \quad (11)$$

其中 E 为比内能,V 为比容,ϕ 为黏性耗散函数,$\vec{q}$ 为热流向量.

由傅里叶导热定律

$$\vec{q}=-k\nabla_\perp T \quad (12)$$

可得:

$$\nabla\cdot\vec{q}=T\cdot\nabla\cdot(\frac{-k\nabla_\perp T}{T})=-[T\nabla\cdot(\frac{k\nabla_\perp T}{T})+\frac{k}{T}(\nabla_\perp T)^2] \quad (13)$$

将公式(11)代入(5)得:

$$\frac{\mathrm{d}E}{\mathrm{d}t}+p\frac{\mathrm{d}V}{\mathrm{d}t}-VT\nabla\cdot(\frac{k\nabla_\perp T}{T})=V\phi+\frac{Vk}{T}(\nabla_\perp T)^2 \quad (14)$$

将 Gibbs 方程 $T\mathrm{d}s=\mathrm{d}E+p\mathrm{d}V$ 代入公式(14)并忽略一阶小量得:

$$\rho_0\frac{\mathrm{d}s}{\mathrm{d}t}-\nabla\cdot(\frac{k\nabla_\perp T_1}{T_0})=\frac{\phi}{T_0}+k(\frac{\nabla_\perp T_1}{T_0})^2 \quad (15)$$

其中 s 为单位体积熵产.

公式(15)左边第一项为单位体积熵产率,第二项为熵流.公式(15)右边第一项为黏性不可逆性引起的熵产率,第二项为传热引起的熵产率.由此可得单位体积熵产率:

$$S_{it}=\frac{\phi}{T_0}+k(\frac{\nabla_\perp T}{T_0})^2 \quad (16)$$

在层流和小扰动条件下,黏性耗散函数为:

$$\phi=\mu(\nabla_\perp u_1)^2 \quad (17)$$

将公式(17)代入公式(16)并取时间平均得:

$$S_{it}=\langle S_{it}\rangle_t=\frac{k}{2T_0^2}(\nabla_\perp T\cdot\nabla_\perp T^*)+\frac{\mu}{2T_0}(\nabla_\perp u\cdot\nabla_\perp u^*) \quad (18)$$

其中 * 表示复共轭.

将公式(7)和公式(8)代入公式(18)并取实部可得针束型回热器时均熵产率:

$$S_{it}=\frac{1}{2T_0^2}[\frac{T_0^2\beta^2a^2u_1^2Z^2\omega\rho_0}{c_p}\mathrm{Re}(M_{11})+(\frac{\mathrm{d}T_0}{\mathrm{d}x})^2\frac{u_1^2\rho_0c_p}{\omega(1-\sigma)^2}\mathrm{Re}(M_{21})+\frac{u_1^2T_0\beta Z\rho_0a\sqrt{\sigma}}{1-\sigma}\frac{\mathrm{d}T_0}{\mathrm{d}x}\mathrm{Im}(M_{31})]+\frac{\omega\rho_0}{2T_0}\cdot u_1^2\cdot F_\mu\cdot F_\mu^* \quad (19)$$

其中

$$\mathrm{Re}(M_{11})=A_{jk}J_1(z_k)A_{jk}^*J_1^*(z_k)+A_{yk}Y_1(z_k)A_{yk}^*Y_1^*(z_k)-2\mathrm{Re}[A_{jk}J_1(z_k)A_{yk}^*Y_1^*(z_k)]$$

$$\mathrm{Re}(M_{21})=A_{jk}J_1(z_k)A_{jk}^*J_1^*(z_k)+A_{yk}Y_1(z_k)A_{yk}^*Y_1^*(z_k)-2\mathrm{Re}[A_{jk}J_1(z_k)A_{yk}^*Y_1^*(z_k)]+\sigma\{A_{j\mu}J_1(z_\mu)A_{j\mu}^*J_1^*(z_\mu)+$$

$$A_{y\mu}Y_1(z_\mu)A_{y\mu}^*Y_1^*(z_\mu) -$$
$$2\mathrm{Re}[A_{y\mu}Y_1(z_\mu)A_{j\mu}^*J_1^*(z\mu)]\} -$$
$$2\sqrt{\sigma}\mathrm{Re}[A_{j\mu}J_1(z_\mu)A_{jk}^*J_1^*(z_k) +$$
$$A_{y\mu}Y_1(z_\mu)A_{yk}^*Y_1^*(z_k) -$$
$$A_{y\mu}Y_1(z_\mu)A_{jk}^*J_1^*(z_k) -$$
$$A_{j\mu}J_1(z_\mu)A_{yk}^*Y_1^*(z_k)]$$

$$\mathrm{Im}(M_{31}) = 2\mathrm{Im}[A_{yk}Y_1(z_k)A_{j\mu}^*J_1^*(z_\mu) +$$
$$A_{jk}J_1(z_k)A_{y\mu}^*Y_1^*(z_\mu) +$$
$$A_{j\mu}J_1(z_\mu)A_{jk}^*J_1^*(z_k) +$$
$$A_{y\mu}Y_1(z_\mu)A_{yk}^*Y_1^*(z_k)]$$

$$F_\mu = \frac{Y_1(z_{0\mu})J_1(z_\mu) - J_1(z_{0\mu})Y_1(z_\mu)}{Y_1(z_{0\mu})J_0(z_{d\mu}) - J_1(z_{0\mu})Y_0(z_{d\mu})}$$

$$A_{jk} = \frac{Y_1(z_{0k})}{Y_1(z_{0k})J_0(z_{dk}) - J_1(z_{0k})Y_0(z_{dk})}$$

$$A_{yk} = \frac{J_1(z_{0k})}{Y_1(z_{0k})J_0(z_{dk}) - J_1(z_{0k})Y_0(z_{dk})}$$

$$A_{j\mu} = \frac{Y_1(z_{0\mu})}{Y_1(z_{0\mu})J_0(z_{d\mu}) - J_1(z_{0\mu})Y_0(z_{d\mu})}$$

$$A_{y\mu} = \frac{J_1(z_{0\mu})}{Y_1(z_{0\mu})J_0(z_{d\mu}) - J_1(z_{0\mu})Y_0(z_{d\mu})}$$

其中 σ 为工质 Prandtl 数,阻抗比 $Z = \frac{p_1(x)}{\rho_0 a u_1(x)}$.

由公式(19)可知 S_{ir}与 r 有关,即 S_{ir}沿流道横向截面有一分布,取其截面平均得:

$$S_i = (S_{ir})_r = \frac{1}{\pi(r_0^2 - r_d^2)}\int_{rd}^{r0} 2\pi r S_{ir}\mathrm{d}r =$$
$$\frac{1}{2T_0^2}[\frac{T_0^2\beta^2 C_0^2\mu_1^2 Z^2\omega\rho_0}{c_p}F_1 + (\frac{\mathrm{d}T_0}{\mathrm{d}x})^2\frac{u_1^2\rho_0 c_p}{\omega(1-\sigma)^2}F_2$$
$$-\frac{u_1^2 T_0\beta Z\rho_0 C_0\sqrt{\sigma}}{1-\sigma}\frac{\mathrm{d}T_0}{\mathrm{d}x}F_3] + \frac{\omega\rho_0}{2T_0}u_1^2 F_4 \qquad (20)$$

其中

$$F_1 = \frac{1}{\pi(r_0^2 - r_d^2)}\int_{rd}^{r0} 2\pi r\mathrm{Re}(M_{11})\mathrm{d}r =$$
$$\frac{2}{r_0^2 - r_0^2}[A_{jk}A_{jk}^*M + J_{1K}J_{1K}^* + A_{yk}A_{yk}^*M_{Y_{1k}Y_{1k}^*} -$$
$$\mathrm{Re}(A_{jk}A_{yk}^*M_{J_{1k}Y_{1k}^*})]$$

$$F_2 = \frac{1}{\pi(r_0^2 - r_d^2)}\int_{r_d}^{r_0} 2\pi r\mathrm{Re}(M_{21})\mathrm{d}r =$$
$$\frac{2}{r_0^2 - r_d^2}\{A_{jk}A_{jk}^*M_{J_{1k}J_{1k}^*} + A_{yk}A_{yk}^*M_{Y_{1k}Y_{1k}^*} -$$
$$2\mathrm{Re}(A_{jk}A_{yk}^*M_{J_{1k}Y_{1k}^*}) + \sigma[A_{j\mu}A_{j\mu}^*M_{J_{1\mu}J_{1\mu}^*} +$$
$$A_{y\mu}A_{y\mu}^*M_{Y_{1\mu}Y_{1\mu}^*} - 2\mathrm{Re}(A_{y\mu}A_{j\mu}^*M_{Y_{1\mu}J_{1\mu}^*})]$$
$$-2\sqrt{\sigma}\mathrm{Re}(A_{j\mu}A_{jk}^*M_{J_{1\mu}J_{1k}^*} + A_{y\mu}A_{yk}^*M_{Y_{1\mu}Y_{1k}^*} -$$
$$A_{y\mu}A_{jk}^*M_{Y_{1\mu}J_{1k}^*} - A_{j\mu}A_{yk}^*M_{J_{1\mu}Y_{1k}^*})\}$$

$$F_3 = \frac{1}{\pi(r_0^2 - r_d^2)}\int_{rd}^{r0} 2\pi r\mathrm{Re}(M_{31})\mathrm{d}r =$$
$$\frac{4}{r_0^2 - r_d^2}\mathrm{Im}(A_{yk}A_{j\mu}^*M_{Y_{1k}J_{1\mu}^*} + A_{jk}A_{y\mu}^*M_{J_{1k}Y_{1\mu}^*} +$$
$$A_{j\mu}A_{jk}^*M_{J_{1\mu}J_{1k}^*} + A_{y\mu}A_{jk}^*M_{Y_{1\mu}Y_{1k}^*})$$

$$F_4 = \frac{1}{\pi(r_0^2 - r_d^2)}\int_{rd}^{r0} 2\pi r F_\mu \cdot F_\mu^*\mathrm{d}r =$$
$$\frac{2}{r_0^2 - r_d^2}(A_{j\mu}A_{j\mu}^*M_{J_{1\mu}J_{1\mu}^*} - A_{j\mu}A_{y\mu}^*M_{J_{1\mu}Y_{1\mu}^*} -$$
$$A_{y\mu}A_{j\mu}^*M_{Y_{1\mu}J_{1\mu}^*} + A_{y\mu}A_{y\mu}^*M_{Y_{1\mu}Y_{1\mu}^*})$$

$$M_{N_{1\eta}R_{1\zeta}} = \int_{rd}^{r0} rN_{1\eta}R_{1\zeta}^*\mathrm{d}r =$$
$$\frac{B_\eta r_d N_0(B_\eta \cdot r_d)R_1(B_\zeta^* \cdot r_d)}{B_\eta^2 - B_\zeta^{*2}} -$$
$$\frac{B_\zeta^* \cdot r_d N_1(B_\eta \cdot r_d)R_0(B_\zeta^* \cdot r_d)}{B_\eta^2 - B_\zeta^{*2}}$$
$$(N, R = J, Y;\ \eta, \zeta = \mu, k)$$

$$B_k = \frac{i-1}{\delta_k}$$

$$B_\mu = \frac{i-1}{\delta_\mu}$$

2 数值结果分析

根据公式(19)和(20),可分析得出不同参数对熵产率的影响:

2.1 截面分布熵产率

公式(19)表明截面分布不可逆熵产率 S_{ir}是针束距中心点距离 r 的函数. 计算时所取参数 $T_0 = 600$ K, $T_0\beta = 1$, $f = \omega/2\pi = 400$ Hz, $\mathrm{d}T/\mathrm{d}x = 1\,000$ K/m, $Z = 1$, $r_d = 0.000\,1$ m, $\rho_0 = 1.9$ kg/m^3, $\sigma = 0.68$和 k = 0.13 $W/(m^2 \cdot K)$. 由图 2 可知:在不同的 r_0/r_d 下 S_{ir}随着 r 的增大而减小. 这是因为离针束越远,换热与黏性耗散的程度越小,回热器的不可逆性越小.

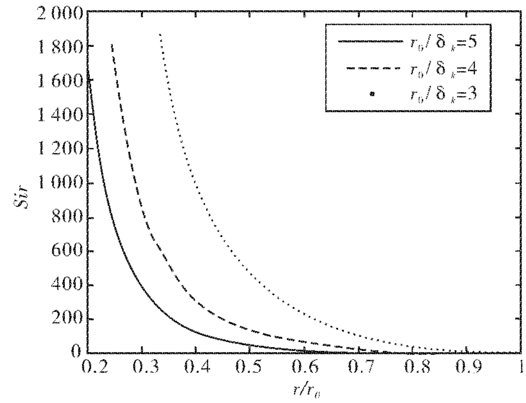

图 2 熵产率的截面分布

Fig. 2 Cross-section entropy generation rate distribution

2.2 温度梯度对截面平均分布熵产率的影响

取参数 $T_0 = 600$ K, $T_0\beta = 1$, $f = \omega/2\pi = 400$

Hz，$Z=1$，$r_d=0.0001$ m，$\rho_0=1.9$ kg/m^3，$\sigma=0.68$ 和 $k=0.13$ W/(m^2·K)，如图 3 所示：在不同 r_0/r_d 时S_{ir}随温度梯度 dT/dx 的增大而增大，这是由于换热导致的不可逆性受温度梯度影响.

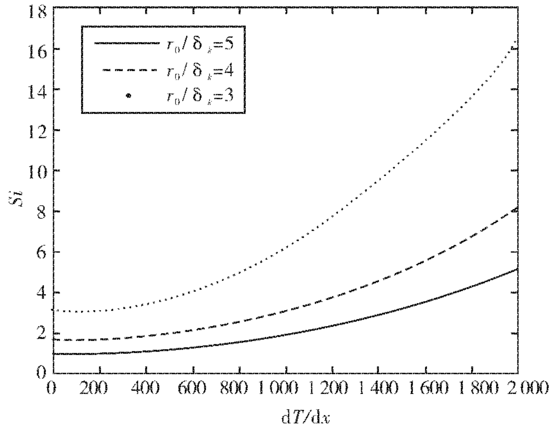

图 3　截面平均熵产率随温度变化规律

Fig. 3　Cross section average entropy generation rate versus temperature gradient

2.3　针束型回热器的优化频率

给定特征尺寸 r_0/δ_k 和 r_d/r_0 时，当角频率 ω 变化时，存在最小截面平均熵产率 S_i. 由公式(20)，当 $\partial S_i/\partial\omega=0$ 时可得：

$$\omega_0=\left[\frac{\left(\frac{dT_0}{dx}\right)^2\cdot c_p^2F_2}{(T_0c_pF_4+T_0^2\beta^2C_0^2Z^2F_1)(1-\sigma)^2}\right]^{\frac{1}{2}} \tag{21}$$

ω_0 为截面平均不可逆熵产率最小时的优化角频率. 计算时取参数 $T_0=600$ K，$T_0\beta=1$，dT/dx = 1 000 K/m，$Z=1$，$r_d=r_0/5$，$\rho_0=1.9$ kg/m^3，$\sigma=0.68$和 $k=0.13$ W/(m^2·K)，在不同 r_0/r_d 时 S_{ir} 随 ω 的变化规律如图 4 所示.

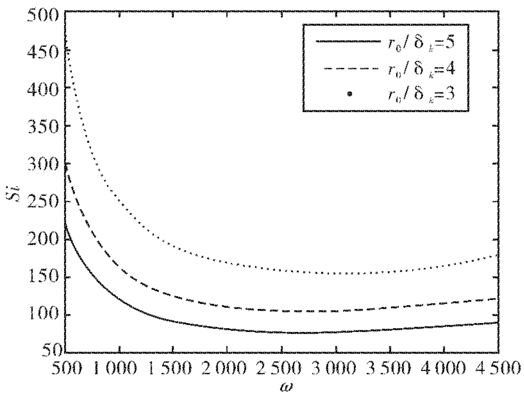

图 4　截面平均熵产率随角频率的变化规律

Fig. 4　Cross section average entropy generation rate versus the circular frequency

优化频率 f_0 经计算可得：

$$f_0=\frac{\omega_0}{2\pi}=\begin{cases}434\ \text{Hz}\ (\frac{r_0}{\delta_k}=3)\\425\ \text{Hz}\ (\frac{r_0}{\delta_k}=4)\\423\ \text{Hz}\ (\frac{r_0}{\delta_k}=5)\end{cases}$$

2.4　针束型回热器的优化阻抗比

取参数 $T_0=600$ K，$T_0\beta=1$，$f=\omega/2\pi=400$ Hz，dT/dx = 1 000 K/m，$r_d=0.0001$ m，$\rho_0=1.9$ kg/m^3，$\sigma=0.68$ 和 $k=0.13$ W/(m^2·K)，在不同 r_0/r_d 时 S_{ir}随阻抗比 Z 的变化规律如图 5 所示. 当 Z 变化时存在最小 S_i，对应的最优 Z 为：

$$Z_0=\begin{cases}0.34\ (\frac{r_0}{\delta_k}=3)\\0.35\ (\frac{r_0}{\delta_k}=4)\\0.36\ (\frac{r_0}{\delta_k}=5)\end{cases}$$

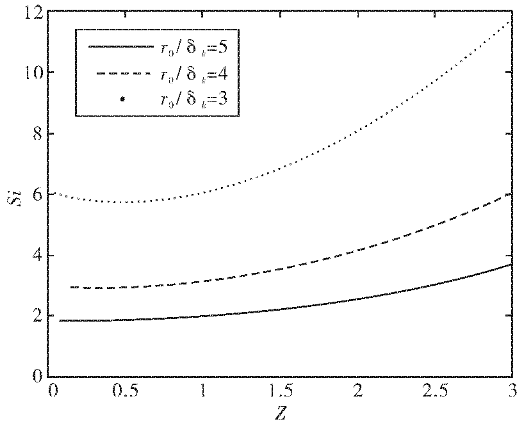

图 5　截面平均熵产率随阻抗比的变化规律

Fig. 5　Cross section average entropy generation rate versus impedance ratio

3　结　语

本文对针束型回热器中由于换热和黏性耗散的不可逆性导致的熵产率进行了研究，计算获得了截面熵产率的分布. 在给定参数下，截面平均分布熵产率随温度梯度的增大而增大，随阻抗比变化时存在最小值. 给定特征尺寸时，获得了最小熵产率对应的最优频率. 本文结果有利于选择针束型回热器的优化尺寸.

参考文献：

[1]　吴锋，李青，郭方中，等. 热声理论的研究进展[J]. 武汉工程大学学报，2012，34(1)：1-6.

[2] Swift G W. Thermoacoustic engines[J]. J Acoust Soc Am, 1984, 84(4): 1145-1180.

[3] Tominaga A. Thermodynamic aspects of thermoacoustic theory[J]. Cryogenics, 1995, 35(7): 427-440.

[4] Hofler T J. Thermoacoustic refrigerator design and performance [D]. San Diego: Physics Department, University of California at San Diego, 1986.

[5] Swift G W. Analysis and performance of a large thermoacoustic engine[J]. J Acoust Soc Am, 1992, 92 (3): 1551-1563.

[6] Swift G W, Keolian R M. Thermoacoustics in pin-array stacks [J]. J Acoust Soc Am, 1993, 94 (2): 941-943.

[7] Hayden M E, Swift G W. Thermoacoustic relaxation in a pin-array stack[J]. J Acoust Soc Am, 1997, 102 (5): 2714-2721.

[8] Gibson R J, Nessler F S, Keolian R M. Measurements of a thermoacoustic pin stack[J]. J Acoust Soc Am, 1996, 100(4): 2735-2742.

[9] Bejan A. The thermodynamic design of heat and mass transfer processes and devices [J]. Heat and Fluid Flow, 1987, 8(4): 398-406.

[10] Bejan A. Entropy generation through heat and fluid flow[M]. New York: Wiley, 1982.

[11] Shohel Mahmud, Roydon Andrew Fraser. The Thermoacoustic irreversibility for a single-plate thermoacoustic system[J]. International Journal of Heat and Mass Transfer. 2006, 49: 3448-3461.

[12] Hadi Babaei, Kamran Siddiqui. Design and optimization of thermoacoustic devices[J]. Energy Conversion and Management, 2008, 49: 3585-3598.

[13] Ishikawa H, Hobson P A. Optimisation of heat exchanger design in a thermoacoustic engine using a second law analysis[J]. Heat mass transfer, 1996, 23(3): 325-334.

[14] 吴锋，陈林根，孙丰瑞，等. 斯特林机的有限时间热力学优化[M]. 北京：化学工业出版社，2008.

[15] 余仕成. 平板型回热器的不可逆熵产率分析[J]. 武汉化工学院学报，1999，21(2)：85-89.

[16] 余仕成，王克协，吴锋. 钢丝型回热器的不可逆熵产率分析[J]，吉林大学自然科学学报，1999，3：52-56.

Analysis of entropy generation rate in pin-array stack

YANG Zhi-chun[1], ***WU Feng***[2], ***YU Shi-cheng***[2]

(1 Navy Representative Office of 438 Factory, Wuhan 430064, China;
2 School of Science, Wuhan Institute of Technology, Wuhan 430074, China)

Abstract: The stack is the key element of thermoacoustic engines, and pin-array stack has excellent performance compared with other stack geometries. In the case of parameters optimization of pin-array stack, a minimum entropy generation rate optimization model was established to study parametric optimization of stack based on irreversibility. Based on the analysis of the thermodynamic irreversibilities produced by heat transfer and viscous dissipation, the theoretical study and the numerical calculation on entropy generation rate in pin-array stack with the oscillating working gas have been done. Cross-section entropy generation rate distribution and cross-section average entropy generation rate were obtained, the variation law of entropy generation rate in different cross-section of pin-array stack was analyzed, and effect of temperature gradient on cross-section average entropy generation rate was studied. For the fixed characteristic dimension and the minimum cross-section average entropy generation rate, the optimization frequency and the optimization impedance ratio were obtained.

Key words: entropy generation rate; optimization frequency; pin-array stack; thermoacoustic; irreversibility

本文编辑：龚晓宁